ISSN 1027-5495. Functional Materials, 30, No.1 (2023), p. 5-11.
doi:https://doi.org/10.15407/fm30.01.5

Enhancement of scintillation characteristics by doping $ZnWO_4$ crystals

I.Tupitsyna, A.Dubovik, V.Alekseev

Institute for Scintillation Materials, National Academy of Sciences of Ukraine, 60 Nauky Ave., 61072 Kharkiv, Ukraine

Received December 12, 2022

The influence of doping on the luminescent and scintillation parameters of zinc tungstate crystals was investigated. The reasons for the deterioration of the scintillation characteristics of $ZnWO_4$ caused by molybdenum impurities are discussed. Ways of obtaining scintillators based on $ZnWO_4$ doped with Me^{1+} and Me^{3+} and fluorine compounds with improved scintillation parameters are proposed.

Keywords: zinc tungstate, light output, afterglow, dopants, luminescence, defects.

Поліпшення сцинтиляційних характеристик при легуванні кристалів $ZnWO_4$.
І.А.Туніцина, О.М.Дубовик, В.Д.Олексєєв

Проведено дослідження впливу легування на люмінесцентні та сцинтиляційні параметри кристалів вольфрамата цинку. Обговорюються причини погіршення сцинтиляційних характеристик $ZnWO_4$, викликаних домішкою молібдену. Запропоновано шляхи отримання сцинтиляторів на основі $ZnWO_4$, легованих Me^{1+} та Me^{3+} та сполуками фтору, з поліпшеними сцинтиляційними параметрами.

1. Introduction

A single crystal of cadmium tungstate is actively used as a scintillator for detecting X-rays and γ-rays [1–4]. The zinc tungstate crystal ($ZnWO_4$) has the same crystal structure (space group P2/C) as $CdWO_4$. Their luminescence spectra are in the region where it is convenient to use both photomultipliers and photodiodes as radiation detectors. In addition, zinc tungstate does not contain toxic elements, unlike cadmium tungstate. The high density, thermal and mechanical strength, non-hygroscopicity, short radiation length, and low afterglow in the millisecond range of $ZnWO_4$ make it promising for radiation monitoring systems and digital radiography, high energy physics and other areas of scintillation technology, where cadmium tungstate is already used.

In addition to physical and chemical parameters of scintillation materials, their price, which is mainly determined by the cost of raw materials, is of great importance. One of the ways to improve the functional characteristics of the scintillator is the use of high-purity raw materials, which cost, however, is rapidly increasing. To obtain scintillation materials, raw materials with 99.99 % and higher purity are usually used, but it is also possible to improve the functional parameters of lower quality materials by doping [5–12]. As a result, scintillation materials with all necessary characteristics can be obtained for relatively low cost.

It was previously shown that Mo [13,14] and Fe [15] impurities, as well as intrinsic defects, such as oxygen vacancies [16], form additional low-energy luminescence bands in $ZnWO_4$. The presence of external channels of radiative relaxation of electronic excitations usually leads to the suppression of intrinsic luminescence and a decrease in light output. Impurities and intrinsic defects also form capture centers that can lead to long-lasting afterglow or coloration. The molybdenum impurity is a companion in tungsten compounds and, as a rule, can

Table 1. Impurity composition of the raw material

Sample raw material	The content of impurities, wt.%									
	Fe	Cu	Mn	Mg	Al	Mo	Si	Pb	Ni, Cr, Bi, Ti, Sn	Ca
WO_3 5*N*	$1{\cdot}10^{-4}$	$2{\cdot}10^{-5}$	$<2{\cdot}10^{-5}$	$<5{\cdot}10^{-5}$	$1{\cdot}10^{-4}$	$<2{\cdot}10^{-4}$	$<2{\cdot}10^{-3}$	$<1{\cdot}10^{-4}$	$\cdot10^{-5}$	–
ZnO 5*N*	$1.5{\cdot}10^{-4}$	$\cdot10^{-5}$	$<2{\cdot}10^{-5}$	$3{\cdot}10^{-5}$	$2{\cdot}10^{-4}$	$<5{\cdot}10^{-5}$	$<2{\cdot}10^{-3}$	$<1{\cdot}10^{-4}$	$<5{\cdot}10^{-5}$	$<5{\cdot}10^{-4}$
WO_3 4*N*	$1.5{\cdot}10^{-4}$	$2{\cdot}10^{-3}$	$<2{\cdot}10^{-5}$	$5{\cdot}10^{-5}$	$2{\cdot}10^{-4}$	$2{\cdot}10^{-4}$	$<2{\cdot}10^{-3}$	$<1{\cdot}10^{-4}$	$<5{\cdot}10^{-5}$	–
ZnO 4*N*	$2{\cdot}10^{-4}$	$<2{\cdot}10^{-5}$	$<2{\cdot}10^{-5}$	$1{\cdot}10^{-4}$	$5{\cdot}10^{-4}$	$5{\cdot}10^{-4}$	$<2{\cdot}10^{-3}$	$1{\cdot}10^{-4}$	$<5{\cdot}10^{-5}$	$2{\cdot}10^{-3}$
$ZnWO_4$ 3*N*	$3{\cdot}10^{-4}$	$<3{\cdot}10^{-4}$	$<3{\cdot}10^{-4}$	$4{\cdot}10^{-3}$	$7{\cdot}10^{-4}$	$4{\cdot}10^{-2}$	$<2{\cdot}10^{-3}$	$<3{\cdot}10^{-4}$	$<3{\cdot}10^{-4}$	$<3{\cdot}10^{-4}$

be found in tungstate crystals. In this regard, the role of molybdenum admixture in single crystals of tungstates was studied in many works [13, 14, 17–20], but ways of improving the scintillation characteristics were not considered. Also, intrinsic defects are formed in the zinc tungstate lattice, for example, W^{5+} centers, O^- centers, and oxygen vacancies and their associates, which can worsen the scintillation parameters [21–23].

In this work, possible ways of improving the scintillation characteristics of $ZnWO_4$ single crystals due to doping and co-doping were investigated and crystals with improved scintillation parameters were obtained.

2. Experimental

Single crystals from stoichiometric raw materials of different purity (Table 1) were obtained and doped with mono- or trivalent cations and fluorine anions to study the influence of doping on the optical characteristics of $ZnWO_4$ crystals. The single crystals of zinc tungstate were grown by the Czochralski method from a melt in a platinum crucible under air atmosphere using an induction-heated furnace. The automated control of crystal growth was organized through the use of a weight sensor. A small $ZnWO_4$ crystal, oriented along the [010] direction was used as a seed.

The scintillation characteristics of samples of 10×10×10 mm^3 $ZnWO_4$ crystals were measured relative to a $CdWO_4$ single crystal standard of this size. Luminescence and afterglow were studied for samples 10×10×2 mm^3. Scintillations were excited by γ-rays from a ^{137}Cs source (E_γ = 662 keV). A Hamamatsu R1307 photomultiplier was used as a photoreceiver. Radio- and thermally stimulated luminescence (TSL), when excited by γ-radiation of a ^{241}Am source (E_γ = 59.3 keV), was analyzed using a MDR-23 monochromator. To measure TSL curves, the sample was placed in a vacuum thermostat. The heating rate was 0.05 K/s. The relative afterglow was defined as the ratio $I/I_0{\cdot}100$ %, where I is the photodetector current of the Hamamatsu Si PIN S5106 photodiode proportional to the radiation intensity, measured after a predetermined time interval (20 ms) after the completion of the irradiation; I_0 is the current of the photodetector proportional to the emission intensity of the crystal under X-irradiation (150 keV, 0.3 mA).

3. Results and discussion

3.1 Radioluminescence of $ZnWO_4$

The undoped $ZnWO_4$ crystal, which was grown from raw materials with a purity of 5*N*, when excited by γ-radiation of a ^{241}Am source (E_γ = 59.3 keV) at room temperature had an intense band with a maximum at 490 nm (Fig. 1, curve 1). Similar spectra we have obtained for the zinc tungstate crystals with Li, F, WO_3 and La. The radioluminescence of these crystals is described by this band, the relative intensity of which correlates with the value of the light output for different crystals (Tables 2–4). For the zinc tungstate crystals with Eu and Sm in addition to the band with a maximum at 490 nm at the low-energy side of the luminescence spectrum, there are luminescence bands characteristic of Eu^{3+} (Fig. 1, curve 3) and Sm^{3+} [24].

It is known that the intrinsic luminescence of a zinc tungstate crystal has a maximum at 480–500 nm with a decay time of τ ~ 20 μs at T = 300 K. The luminescence band is associated with radiative transitions of electrons from 2*p* O to 5*d* W, traditionally described as the recombination of self-trapped exciton (STE) at WO_6^{6-} complexes [25–27]. Crystals obtained from raw materials with a purity of 3*N* with a high content of molybdenum ($4{\cdot}10^{-2}$ %) (Table 1) had a

Table 2. Influence of doping on the scintillation parameters of the $ZnWO_4$ crystal

#	Raw material purity	Dopants	Light output, % vs $CdWO_4$	Energy resolution, %37Cs (662 keV)	Afterglow, % after 20 msl	Color
1.	4*N*	–	11	23	0.79	Brown
2.	4*N*	WO_3 — 0.05 %	30	15.3	0.031	Slightly pink
3.	4*N*	WO_3 — 0.05 % Li_2CO_3 — 0.2 %	46	9.8	0.02	Colorless
4.	4*N*	Li_2CO_3 —0.06 % ZnF_2 — 0.6 % WO_3 — 0.05 %	50	8.95	0.002	Colorless
5.	4*N*	LiF — 0.05 %	32	11	0.104	Colorless
6.	4*N*	LiF — 1 % WO_3 — 0.03 %	42	9.6	0.004	Colorless

radioluminescence spectrum different from the spectrum of a pure 5*N* single crystal. It shows a low intensive STE luminescence with a pronounced sideband at 600–700 nm (Fig. 1, curves 1 and 2). Additional low-energy luminescence bands traditionally observed in $ZnWO_4$ were associated with the presence of Mo impurities [13, 14]. The external channels of radiative relaxation of electronic excitations suppress the efficiency of STE luminescence.

When the crystal with a high molybdenum content was excited by UV light (λ = 330 nm), we have observed intense photoluminescence with maximum at ~ 700 nm typical for $ZnWO_4$ crystals with molybdenum impurities. This emission was associated with recombination at the molybdenum luminescent center [25]. Zinc tungstate crystals obtained from raw materials with a high content of molybdenum and doped with Eu2O3 excited by γ-radiation, had STE radioluminescence almost at the level of a pure crystal (Fig. 1, curves 1 and 3). The addition of Eu_2O_3 impurity to a crystal with a high content of molybdenum leads to the suppression of energy transfer to molybdenum centers, which prevents the reduction of STE luminescence.

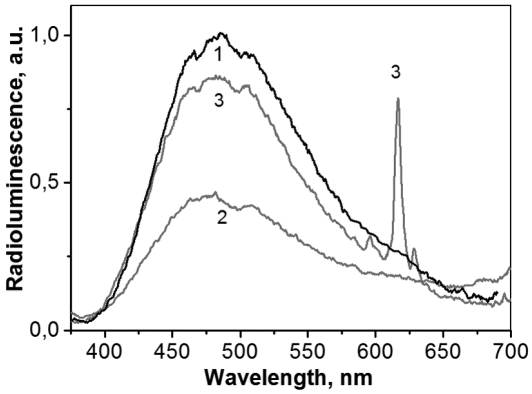

Fig. 1. Radioluminescence spectra of $ZnWO_4$ single crystals: *1* — raw material 5*N*, *2* — raw material 3*N* (Mo — $4 \cdot 10^{-2}$ %), *3* — raw material 3*N* (Mo —$4 \cdot 10^{-2}$ %) with the addition of Eu_2O_3 (1.5 %).

3.2 Thermally stimulated luminescence of $ZnWO_4$

The TSL curves of $ZnWO_4$ single crystals grown from raw materials with a stoichiometric composition of 4*N* purity are presented in Fig. 2. The undoped crystal showed a TSL of low intensity with a small peak at 233 K (curve 1), which was also observed in the crystal with LiF (0.05 %) (curve 2). In addition to this peak, curve 2 also has intense TSL bands at 135, 154, and 176 K. The effect of the dopants containing Li^+ on the TSL of $ZnWO_4$ was investigated from the point of view of changes in structural defects that form charge carrier traps with TSL peaks at temperatures above 160 K. Such traps are responsible for afterglow in the millisecond range. It is known that doping $CdWO_4$ single crystals with lithium compounds leads to the destruction of the capture centers responsible for TSL at temperatures above 160 K [10]. We did not observe this effect for $ZnWO_4$ crystals. Addition of an excess of WO_3 leads to the destruction of the traps responsible for the TSL of 233 K (curves 3 and 4). In the process of $ZnWO_4$ growth, WO_3 is predominantly evaporated, which leads to a deviation from the stoichiometric composition

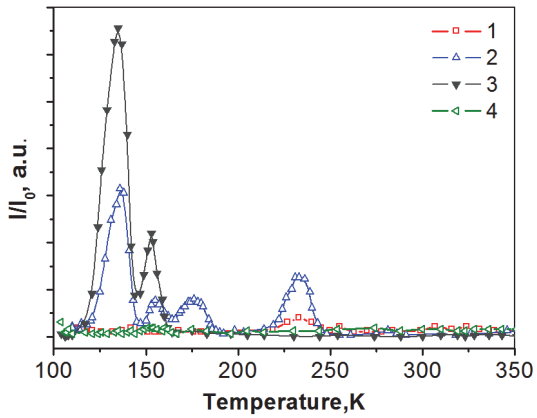

Fig. 2. TSL curves of $ZnWO_4$ single crystals (4*N* raw material with stoichiometric composition): *1* — undoped, *2* — doped with LiF (0.05 %), *3* — doped with LiF (1 %) and WO_3 (0.03 %), *4* — doped with ZnF_2 (0.06 %), Li_2CO_3 (0.06 %) and WO_3 (0.05 %).

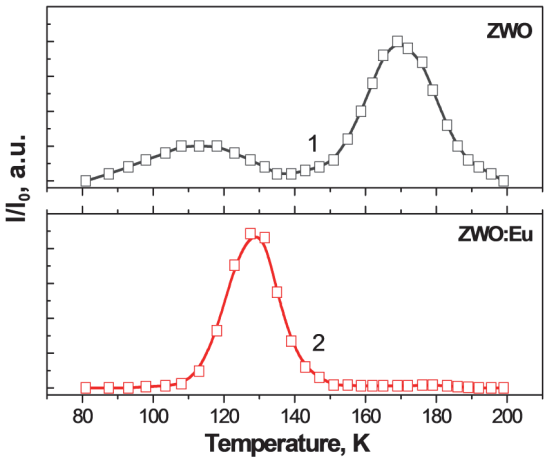

Fig. 3. TSL curves of $ZnWO_4$ single crystals (raw material 3*N* (Mo — $4 \cdot 10^{-2}$ %): *1* — undoped, *2* — doped with Eu_2O_3 (1.5 %).

and the formation of intrinsic defects in the crystal structure, primarily tungsten vacancies and, possibly, associates with these vacancies. Thus, the double doping of LiF (1 %) and WO_3 (0.03 %) provides a crystal with defects that are responsible for TSL only at temperatures lower than 160 K (Fig. 2, curve 3). At the triple doping of $ZnWO_4$ by ZnF_2 (0.06 %), Li_2CO_3 (0.06 %) and WO_3. (0.05 %), no peaks were observed on the TSL curves at temperatures from 77 K to 350 K.

The admixture of molybdenum, which replaces tungsten in the tungstate lattice of $ZnWO_4$, as well as $CdWO_4$, provides traps of charge carriers [13, 14, 18–20], which participate in the recombination process at the molybdenum luminescent center. Two broad non-elemental peaks with maxima at 113 and 170 K are observed on the TSL curve of a $ZnWO_4$ single crystal grown from raw material with a purity of 3N (Fig. 3, curve 1). It was shown in [25] that the spectrum of TSL peaks at temperatures above 150 K corresponds to the luminescence of a molybdenum defect center with a maximum of ~ 700 nm. The luminescence of both molybdenum and STE can be distinguished in the spectral composition of the peaks at lower temperatures. Moreover, the contribution of the STE prevails. When Eu_2O_3 (1.5 %) is added, only one peak with a maximum at 127 K is observed on the TSL curve of the crystal (Fig. 3, curve 2).

3.3 Scintillation parameters and afterglow of $ZnWO_4$

The results of measuring the scintillation parameters of $ZnWO_4$ crystals grown from raw materials of 4*N* and 5*N* purity with the addition of monovalent cations and fluorine anions are in Table 2. The crystals obtained from raw materials of purity 4*N* without additions were brown even after high-temperature air annealing. Experiments have shown that the brown color of $ZnWO_4$ crystals obtained from a charge of stoichiometric composition is due to defects in the crystal lattice, which are created by the preferential evaporation of tungsten oxide from the crucible during the growth process. This effect has a negative impact on the scintillation parameters: low light output of 11 %, energy resolution — 23 %, afterglow level after 20 ms — 0.79 %. It should be noted that in our studies we did not observe a clear correlation between the intensity of TSL at temperatures above 160 K and the value of afterglow after 20 ms. Thus, the undoped crystal from a 4N charge does not store a large amount of light (Fig. 2, curve 1). Perhaps it possesses no TSL in the 300–650 nm spectral range of photodetector used in our measurements (PMT Hamamatsu R1307). However, this crystal has the maximum afterglow of all the crystals we examined (Table 2). The crystal is defective, which is evidenced by intense persistent coloration. It is likely that the crystal stores a fairly large amount of light, but the spectral composition of the TSL is in the sensitivity range of the S5106 photodiode (320–1100 nm), with which we meas-

Table 3. Scintillation parameters of the $ZnWO_4$ crystal grown from raw material with high molybdenum content

#	Raw material purity	Dopants	Light output, % vs $CdWO_4$	Energy resolution, % ^{137}Cs (662 keV)	Afterglow,, % after 20 ms	Color
1.	3*N*	WO_3 — 0.05 % Li_2CO_3 — 0.15 %	18.43	17.55	0.54	Colorless
2.	3*N*	WO_3 — 0.05 % Eu_2O_3 — 1.5 %	33	12.5	0.12	Colorless

ured the afterglow. We observed such an effect in single crystals of $CdWO_4$ doped with Fe [28].

Introduction of an excess of 0.05 wt. % WO_3 helps to reduce the color of the crystal, and the introduction of an excess of WO_3 (0.05 wt.%) and Li_2CO_3 (0.2 wt.%) leads to discoloration of the crystals. Doping $ZnWO_4$ crystals with lithium compounds in combination with zinc fluoride made it possible to improve their scintillation properties. For $ZnWO_4$ crystal samples obtained from 4*N* raw materials, the light output was 50 % relative to the $CdWO_4$ crystal, the energy resolution was 8.5 %, and the afterglow level after 20 ms was 0.002 % (Table 2). This effect is explained by a change in the defect structure of the crystal, which is responsible for the formation of charge carrier traps: monovalent lithium ions compensate for the charge of heterovalent uncontrolled impurities, and fluorine ions, due to its high electronegativity, prevent the reduction of W^{6+} to W^{5+}. It should be emphasized that doping made it possible to significantly reduce (by more than two orders of magnitude) the afterglow of the $ZnWO_4$ crystal. The use of high-purity raw materials (5*N*) made it possible to grow crystals with even higher scintillation parameters — the light output is more than 63 % relative to the $CdWO_4$ crystal, the energy resolution of ^{137}Cs (662 keV) is 8 % (Table 2, Fig. 4).

In the work, an attempt was made to improve the scintillation parameters of $ZnWO_4$ crystals grown from raw materials of lower purity (3*N*) with the content of accompanying tungsten with a molybdenum admixture of about $4 \cdot 10^{-2}$ wt. % (Table 1). Single crystals from this charge are colorless, so their low light output is not related to reabsorption, which we observed for the colored brown crystal (Table 2, #1). But in crystals with molybdenum impurities, defect luminescence centers are formed, which compete with STE, reduce the intensity of

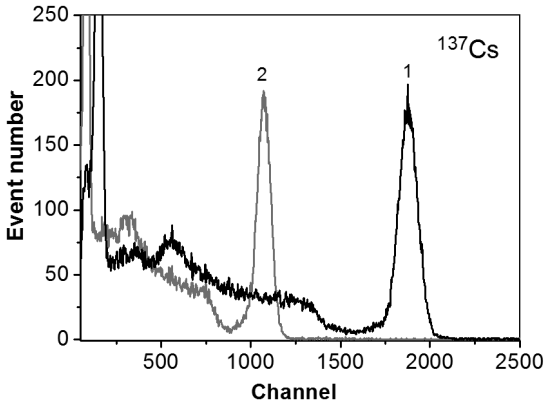

Fig. 4. Amplitude spectra of crystals: *1* — $CdWO_4$ (standard), *2* — $ZnWO_4$ (# 7, Table 2).

scintillation light and increase the decay time. It also leads to the reduction of the light output, because the decay time of radiation associated with defects and impurities, exceeds the time limits of registration by scintillation equipments. In addition, the modification of the spectral composition of scintillation light also negatively affects the light output, because the sensitivity of the PMT is optimized for the main spectral region of the scintillator emission band. The STE radioluminescence of $ZnWO_4$ single crystals with such molybdenum defect centers decreases almost by half. At the same time, we observe low-intensity luminescence of the defect centers in the red part of the spectrum. These centers can be characterized as centers with a low emission probability. The relaxation of the molybdenum centers occurs mainly without radiation due to the transfer of excess energy to the crystal lattice. In this process, molybdenum acts as a quenching center. This was observed for crystals grown from raw materials contaminated with molybdenum. Such samples had a light output more than two times lower than crystals purer in terms of molybdenum (Tables 2, #3). Doping with europium (Table 3, # 2) leads to an increase in light output almost to the level of 4*N* pu-

Table 4. Scintillation parameters of $ZnWO_4$ crystals doped with REE

#	Dopants	Light output, % vs $CdWO_4$	Energy resolution, % ^{137}Cs (662 keV)
1.	–	33.5	15.6
2.	Eu_2O_3 — 0.2 %	41.6	13.1
3.	Eu_2O_3 — 0.5 %	39.5	14.7
4.	Eu_2O_3 — 0.8 %	29.3	15.6
5.	La_2O_3 — 0.1 %	32.0	11.3
6.	La_2O_3 — 0.05 %	41.1	11.2
7.	Sm_2O_3 — 0.05 %	47.7	10.0

rity crystals, and a 5-fold decrease in afterglow. These results correlate with the TSL of these samples. Thus, for an undoped crystal with an uncontrolled impurity, we are talking about an intense peak at T = 170 K (Fig. 3). This confirms the fact that the Mo admixture generates electron traps in $ZnWO_4$ crystals, which partially prevent the transfer of energy to their intrinsic luminescence centers and lead to the appearance of an inertial emission, which leads to an increase in the afterglow level and a decrease in light output. Doping with Eu^{3+} leads to a redistribution of the light sum at the level of a low-temperature peak (127 K), which corresponds to a shorter decay time and the spectral composition of this peak corresponds to the STE. This may explain the improvement of characteristics in the Eu^{3+} doped crystals. The assumption that the 127 K TSL peak is related to intrinsic defects was confirmed in studies of crystals doped with other trivalent rare earth elements. Table 4 shows the scintillation characteristics of a series of crystals, undoped and doped with different concentrations of impurities. It has been shown that the doping of $ZnWO_4$ by 0.05 wt.% of La_2O_3 or Sm_2O_3 in a charge increases the light output of crystals obtained from low-purity raw materials by almost 1.5 times.

4. Conclusions

Comprehensive studies of the effect of doping with mono- and trivalent cations and fluorine compounds on the luminescent and scintillation parameters of zinc tungstate crystals were carried out. Ways of obtaining scintillators based on doped $ZnWO_4$ with improved scintillation parameters are proposed.

It was determined that the doping of $ZnWO_4$ crystals with modifying impurities (Li_2CO_3 ~ 0.06 wt. %, ZnF_2 ~ 0.6 wt. %, WO_3 ~ 0.05 wt. %) allows produce single crystals with improved scintillation characteristics: light output ~ 50 % vs $CdWO_4$, energy resolution 8.5 % with ^{137}Cs excitation (E_γ = 662 keV), afterglow level after 20 ms of 0.002 %.

It was determined that the molybdenum admixture provides defect luminescent centers in the $ZnWO_4$ crystal lattice, which are also quenching centers, and traps of charge carriers, which led to a significant decrease of scintillation parameters and increase of millisecond afterglow. Single crystals of $ZnWO_4$ obtained from a 3N charge with a high content of molybdenum and doped with Eu, La, and Sm, have scintillation parameters at the level of zinc tungstates obtained from raw materials with a purity of 4N.

References

1. Christos Michail, Vaia Koukou, Niki Martini, George Saatsakis et al., *Crystals*, **10**, 429 (2020).
2. R.Deych, J.Dobbs, S.Marcovici et al., in: Proc. Int. Conf. on Inorganic Scintillators and Applications, SCINT'95 (1995), p.36.
3. S.Izumi, S.Kamata, K.Saton et al, *IEEE T. Nucl. Sci.*, **40**, 158 (1991).
4. W.Grabmaier, B.Rossner, *Nucl. Tracks. Rad. Meas.*, **21**, 43 (1991).
5. H.Yamada, A.Suzuki, Y.Uchida et al., *J. Electrochem. Soc.*, **136**, 2713 (1989).
6. C.Michail, I.Valais, I.Seferis et al., *Radiat. Meas.*, **70**, 59 (2014).
7. S.J.Duclos, C.D.Greskovich, R.J.Lyons et al., *Nucl. Instrum. Meth. A*, **505**, 68 (2003).
8. M.Nikl, *Phys. Status. Solidi. A*, **178**, 595 (2000).
9. A.A.Annenkov, M.V.Korzhik, P.Lecoq, *Nucl. Instrum. Meth. A*, **490**, 30 (2002).
10. L.Nagornaya, G.Onyshchenko, E.Pirogov et al., *Nucl. Instrum. Methods*, **A 537**, 163 (2005).
11. M.Buryi, V.V.Laguta, J.Hybler et al., *Phys. Status Solidi B*, **248**, 993-6 (2011).
12. M.Nikl, A.Yoshikawa, *Adv. Opt. Mater.*, **3**, 463 (2015).
13. V.Nagirnyi, L.Jonsson, M.Kirm et al., *Radiat. Meas.*, **38**, 519 (2004).

14. I.Foldvari, L.A.Kappers, O.R.Gilliam et al., *J. Phys. Chem. Solids*, **51**, 953 (1990).
15. L.Grigorieva, D.Millers, S.Chernov et al., *Radiat. Meas.*, **33**, 645 (2001).
16. H.Wang, F.D.Medina, M.S.Antonius et al., *Chem. Phys. Lett.*, **206**, 497 (1993).
17. N.Y.Garces, M.M.Chirila, H.J.Murphy, *J. Phys. Chem. Solids*, **64**, 1195 (2003).
18. O.V.Rzhevskaya, D.A.Spasski, V.N.Kolobanov et al., *Opt. Spectrosc.*, **104**, 366 (2008).
19. A.Kotlov, L.Jonsson, M.Kirm et al., *Radiat. Meas.*, **38**, 715 (2004).
20. A.L.Apanasenko, A.V.Kuznichenko, V.N.Lebedev et al., *Opt. Spectrosc.*, **76**, 868, (1994).
21. Watterich, L.Kovacs, O.R.Gilliam et al., *Radiat. Prot. Dosim.*, **65**, 97 (1996).
22. Watterich, A.Hofstaetter, *Solid. State. Commun.*, **105**, 357 (1998).
23. A.Watterich et al., *J. Phys.: Condens. Matter.*, **13**, 1595 (2001).
24. I.Tupitsyna, A.Dubovik, A.Yakubovskaya et al., *Journal of Crystal Growth*, **586**, 126632 (2022).
25. N.R.Krutyak, V.V.Mikhailin, A.N.Vasil'ev et al., *J. Lumin.*, **144**, 105 (2013).
26. A.E.Ovechkin et al., *Phys. Status. Solidi. A*, **103**, 285 (1987).
27. V.Babin, P.Bohacek, E.Bender et al., *Radiat. Meas.*, **38**, 533 (2004).
28. B.V.Grinyov, Z.T.Moroz, L.L.Nagornaya et al., *Functional Materials*, **12**, 256 (2005).